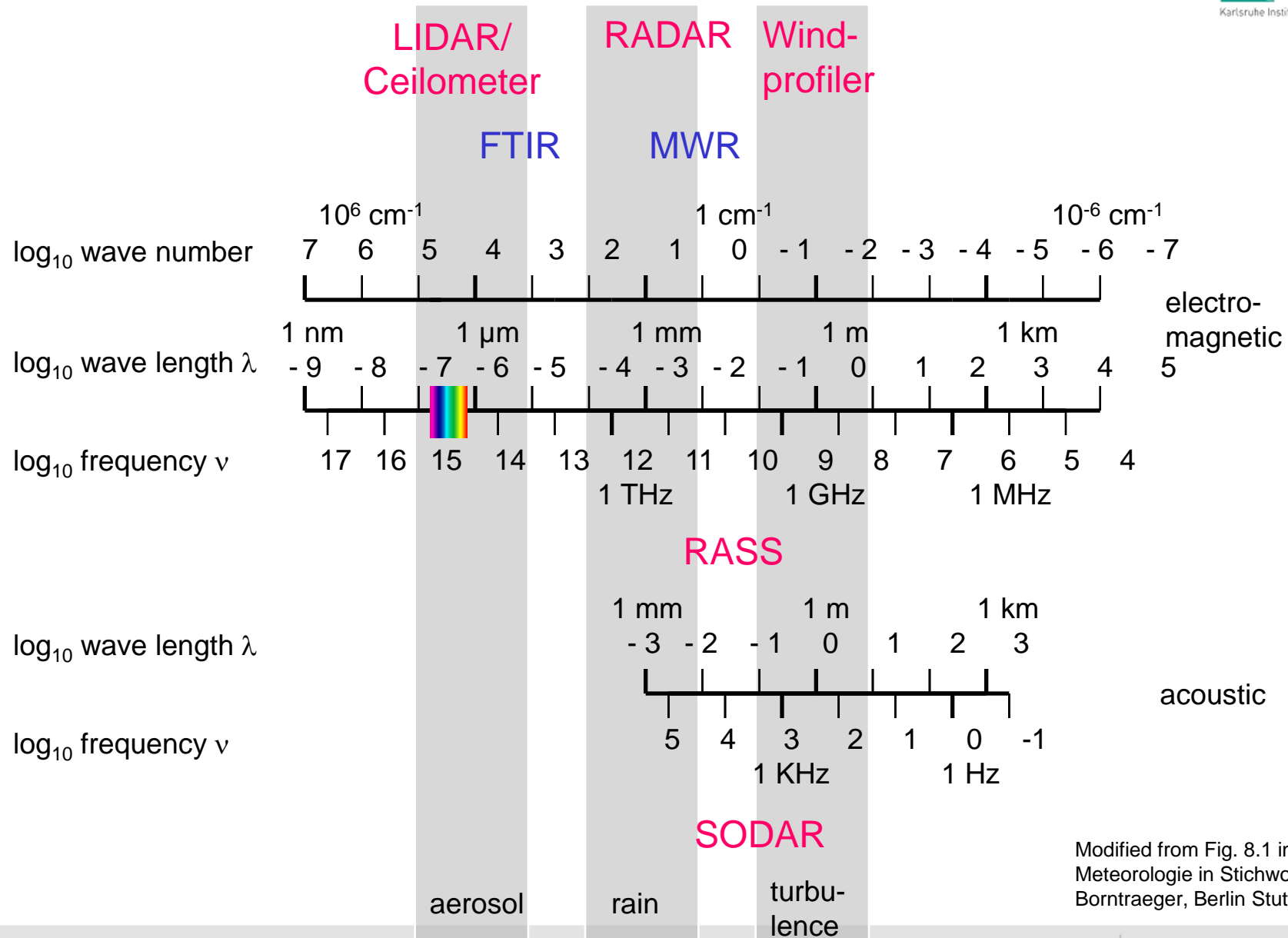


Detection of mixing-layer heights from ground-based remote sensing with SODAR, ceilometers, and RASS – algorithms and experiences

Stefan Emeis

*Institute for Meteorology and Climate Research
Atmospheric Environmental Research Division (IMK-IFU)
Karlsruhe Institute of Technology (KIT)
Kreuzeckbahnstr. 19
82467 Garmisch-Partenkirchen, Germany
E-mail: emeis@kit.edu*

Typical frequency bands for remote sensing of the atmosphere



Modified from Fig. 8.1 in „
Meteorologie in Stichworten“,
Borntraeger, Berlin Stuttgart 2000

Basic remote sensing techniques

name	principle	spatial resolution	direction	type
RADAR	backscatter, electro-magnetic pulses, fixed profiling wave length		scanning, slanted	active, monostatic
SODAR	backscatter, acoustic pulses, fixed wave length	profiling	fixed, slanted, vertical	active, usually monostatic
LIDAR	backscatter, optical pulses, fixed wave length(s)	profiling	scanning, fixed, horizontal, slanted, vertical	active, monostatic
RASS	backscatter, acoustic, electro-magnetic, fixed wave length	profiling	fixed, vertical	active, monostatic
	absorption, infrared, spectrum	path-averaging	fixed, horizontal, slanted	active, bistatic or passive
FTIR	emission, infrared, spectrum	path-averaging	fixed, horizontal, slanted	passive
DOAS	absorption, optical, fixed wave lengths	path-averaging	fixed, horizontal	active, bistatic
radiometry	electro-magnetic, fixed wave length(s)	averaging, profiling	fixed, scanning, slanted, vertical	passive
tomography	travel time, acoustic, fixed wave length	horizontal distribution	fixed, horizontal	active, multiple emitters and receivers

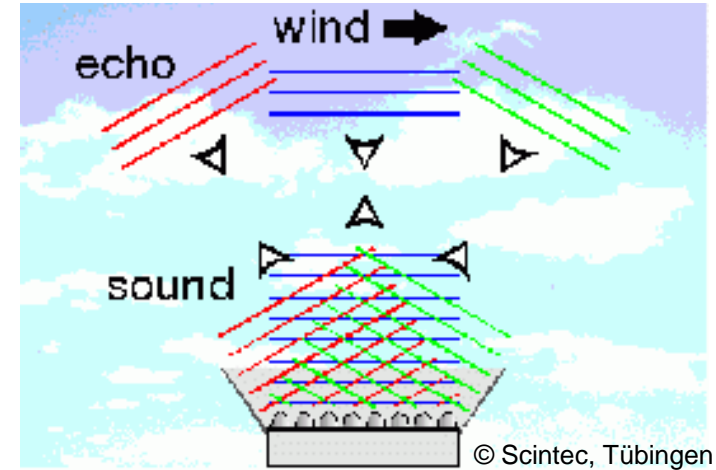
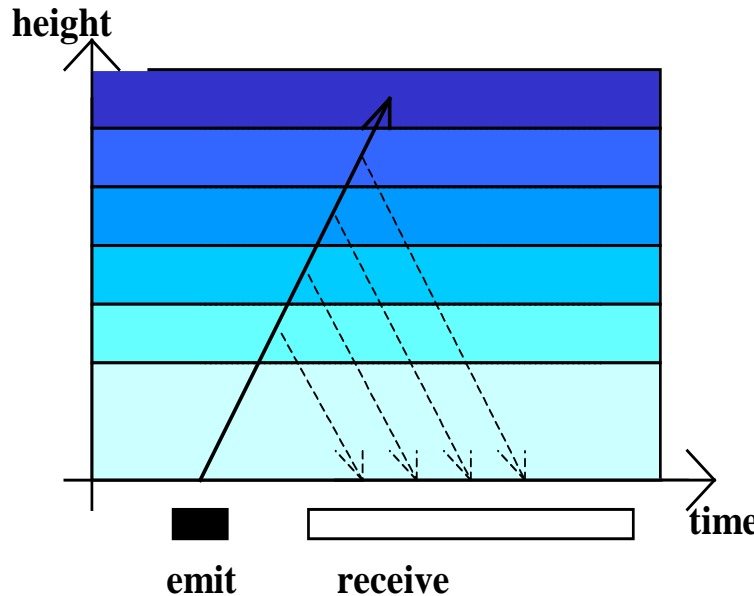
subject of this talk

subject of this talk

SODAR

algorithms for mixing-layer height

monostatic SODAR: measuring principles



deduction:

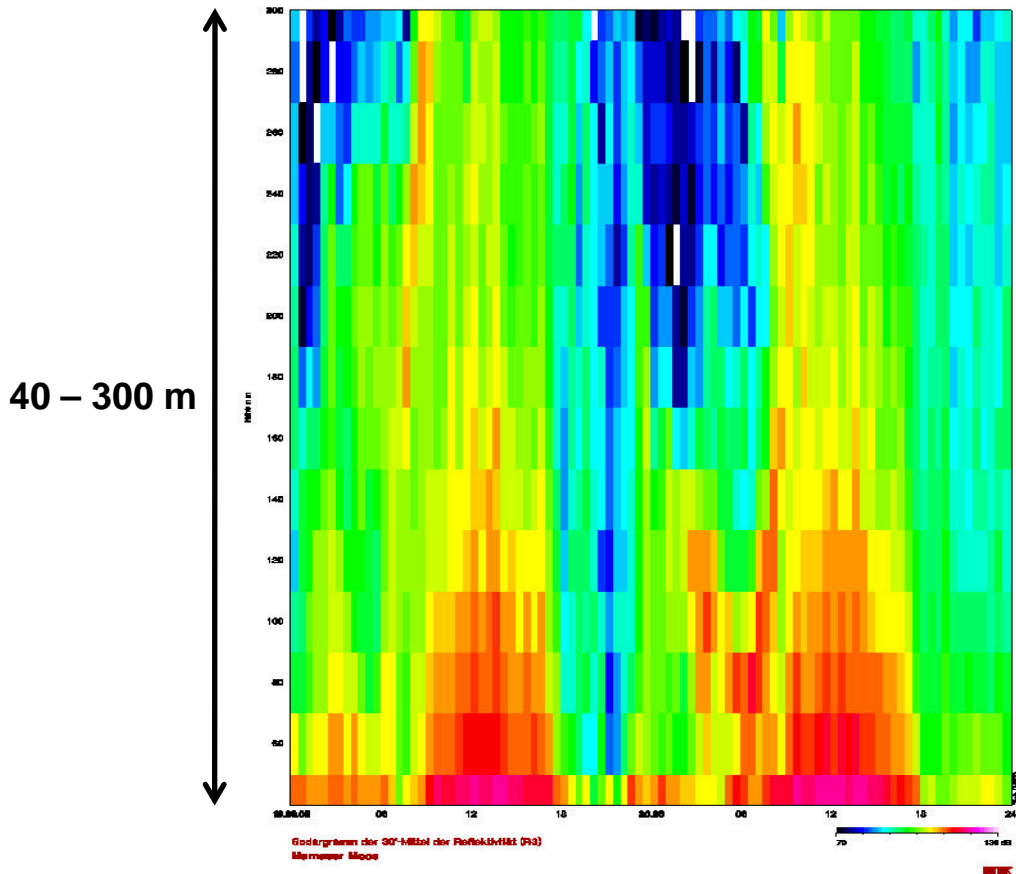
$$\begin{array}{ll}
 \text{sound travel time} & = \text{height} \\
 \text{backscatter intensity} & = \text{turbulence} \\
 \text{Doppler-shift} & = \text{wind speed}
 \end{array}$$

Emission of sound waves
into three directions:

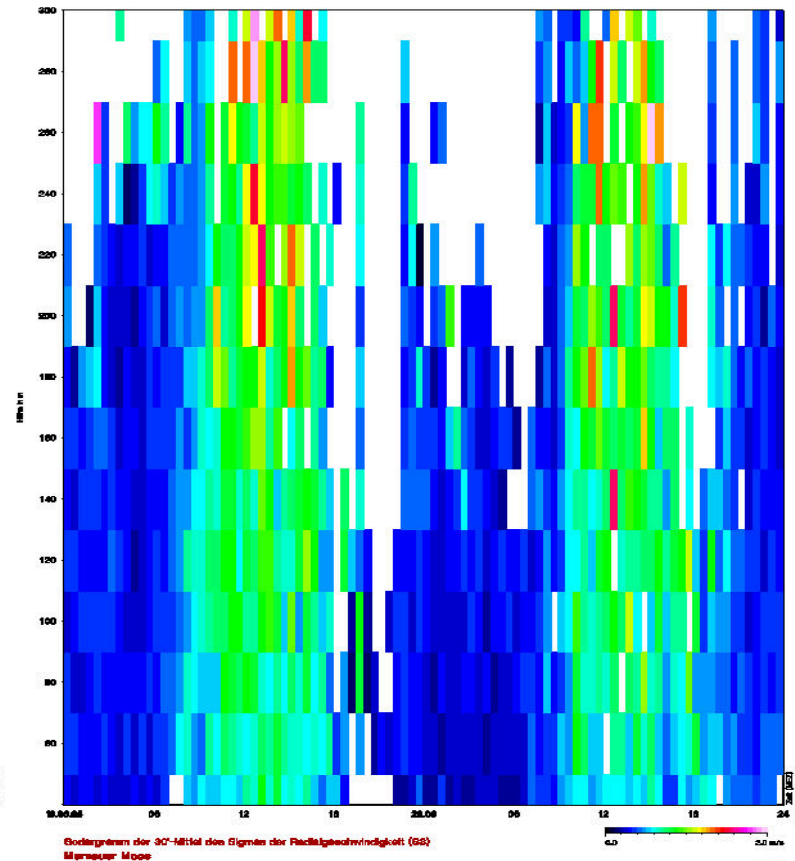
in order to measure all three
components of the wind
(horizontal and vertical)

Sample plot SODAR (convective BL at daytime)

acoustic backscatter intensity

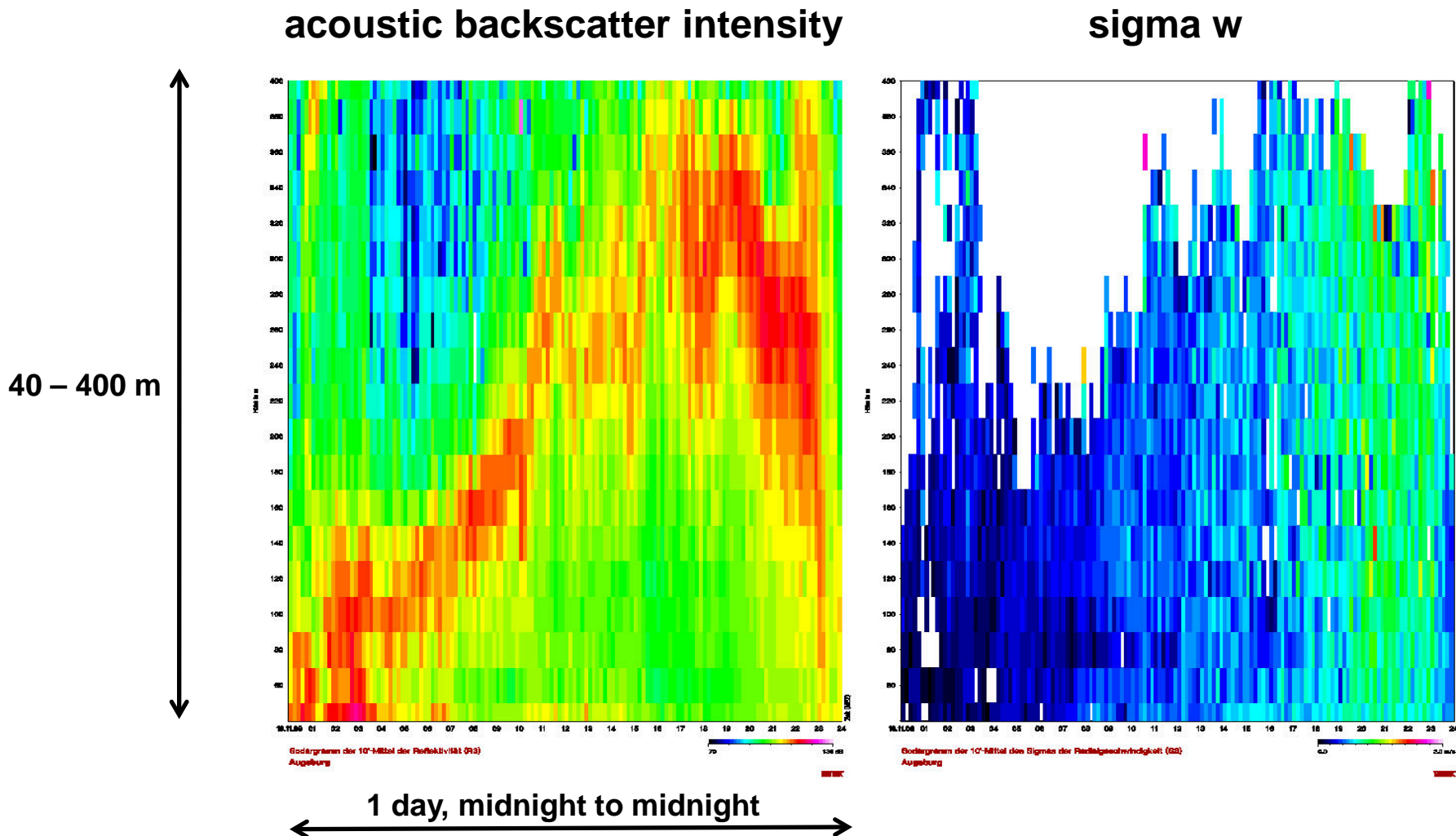


sigma w



2 days, midnight to midnight

Sample plot SODAR (lifted inversion)

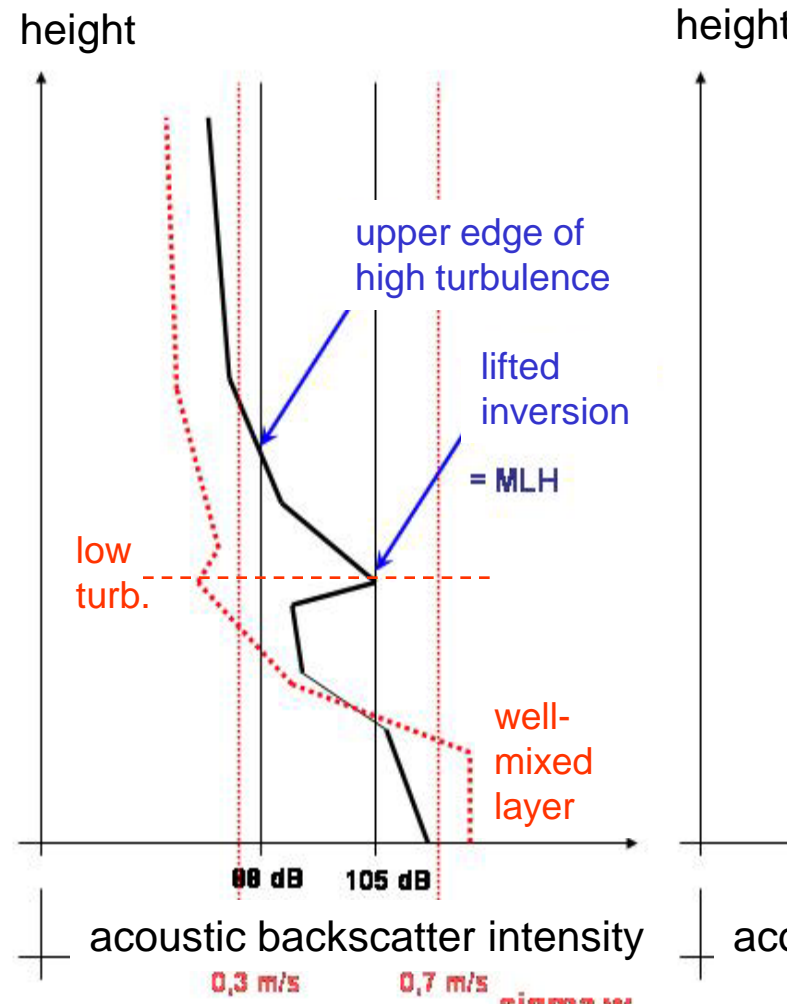


Algorithms to
detect MLH
from SODAR data

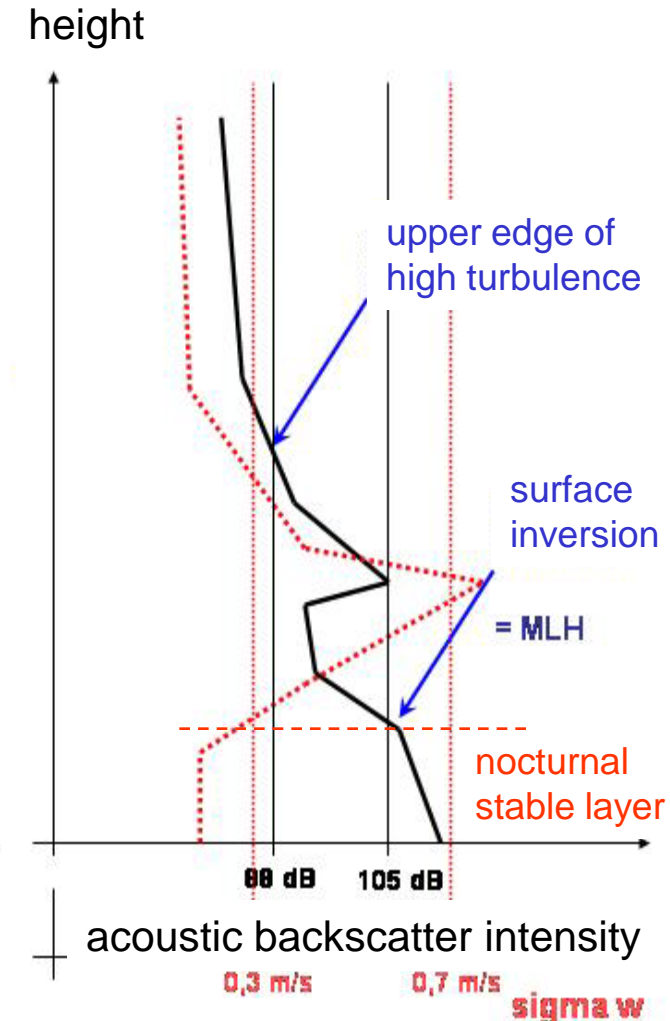
criterion 1:
upper edge
of high
turbulence

criterion 2:
surface and
lifted
inversions

$MLH = \text{Min} (C1, C2)$



example 1: daytime

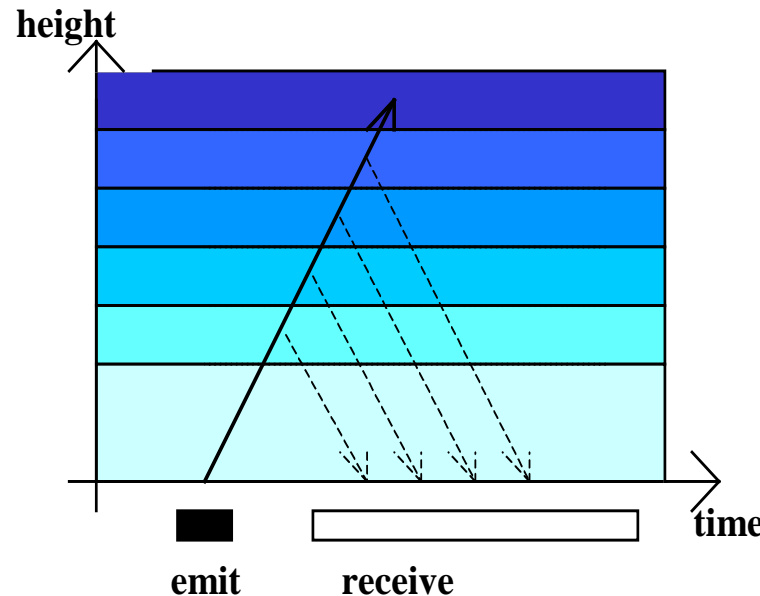


example 2: night-time

Ceilometer

algorithms for mixing-layer height

Ceilometer/LIDAR measuring principle

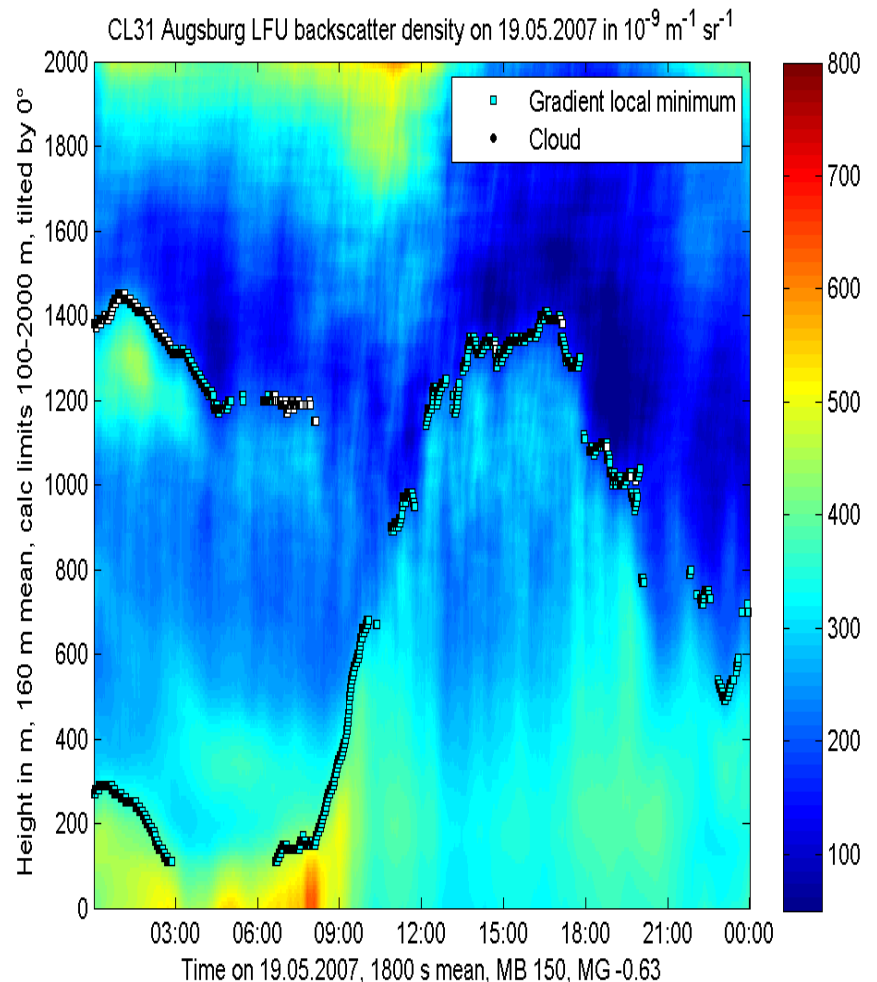


detection:

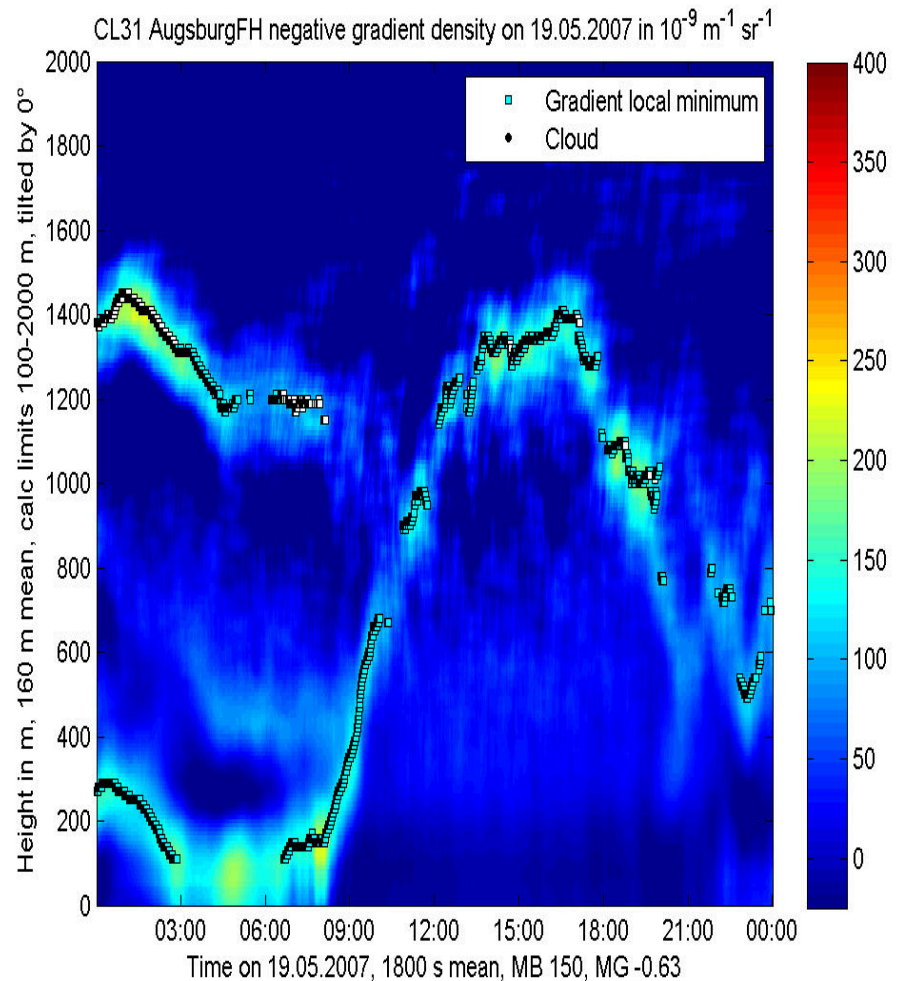
- | | |
|-----------------------|----------------------------------------------------------------------------------------------------------|
| travel time of signal | = height |
| backscatter intensity | = particle size and number distribution |
| Doppler-shift | = cannot be analyzed from ceilometer data
(only from Wind-LIDAR: velocity component in line of sight) |

Sample plot ceilometer (convective BL at daytime)

optical backscatter intensity



negative vertical gradient of optical backscatter intensity

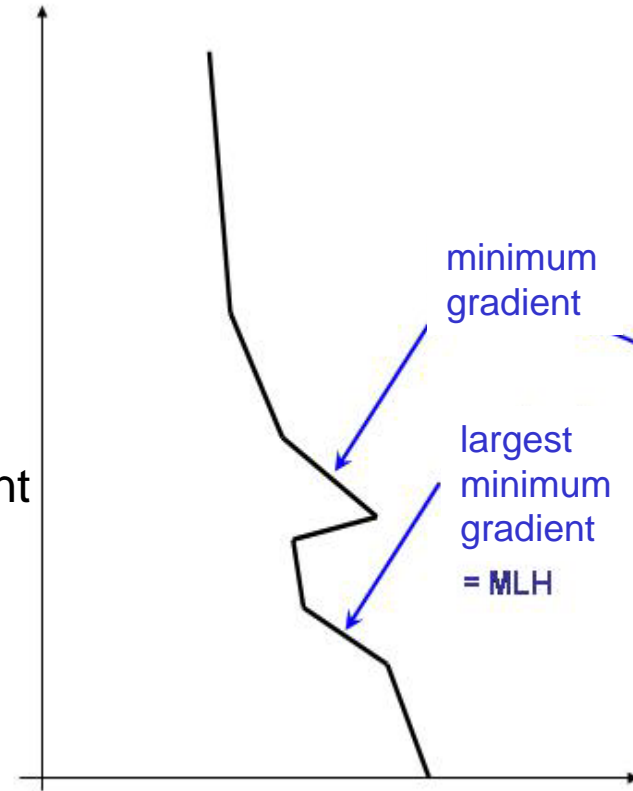


Algorithms to
detect MLH
from Ceilometer-Daten

criterion

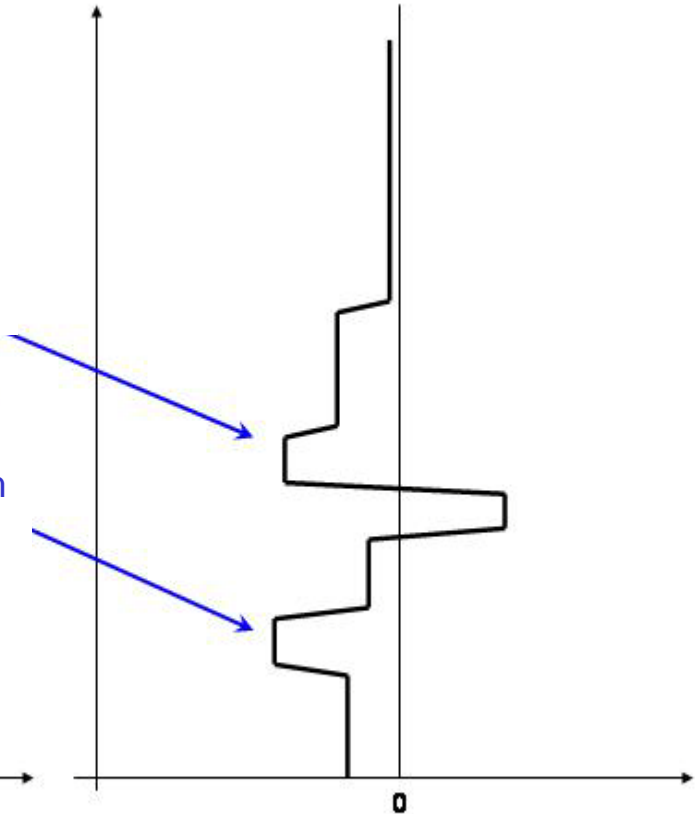
minimal vertical gradient
of backscatter
intensity (the most
negative gradient)

height



optical backscatter intensity

height



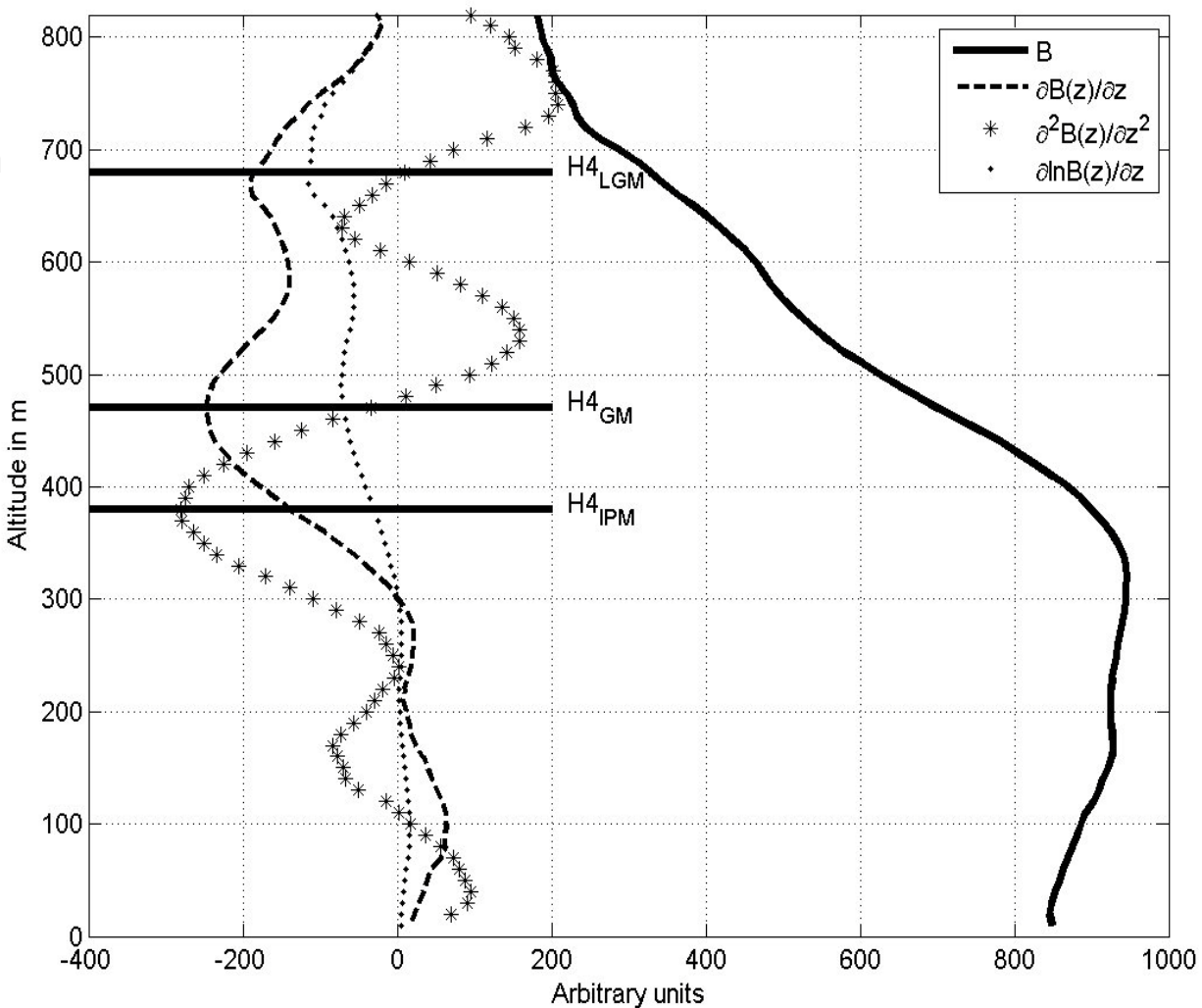
vertical gradient of
optical backscatter intensity

Different gradient methods (see Sicard et al. 2006, BLM 119, 135-157)

logarithmic gradient minimum

gradient minimum

inflection point method
(minimum of 2nd derivative)



comparison of two different ceilometers

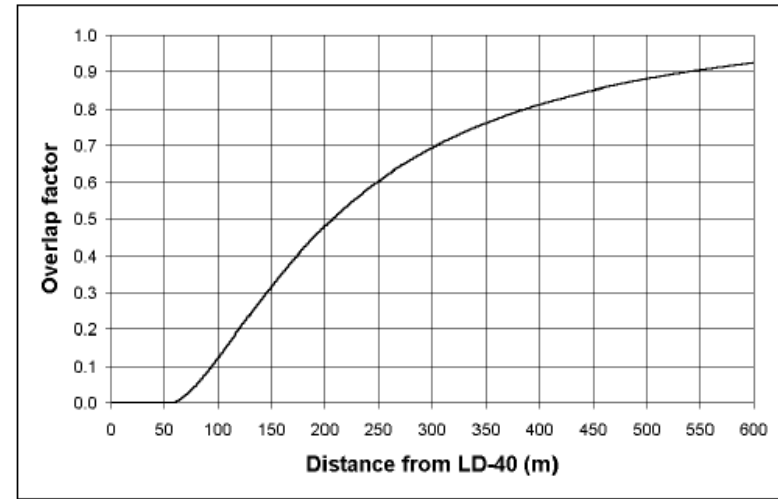
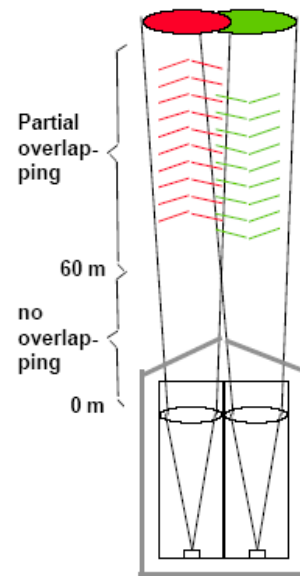
LD40

two optical axes

wave length: 855 nm

height resolution: 7.5 m

max. range: 13000 m



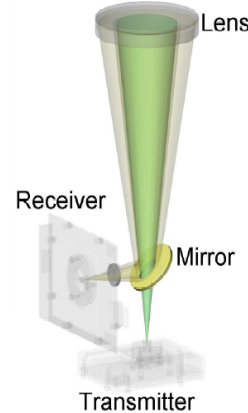
CL31

one optical axis

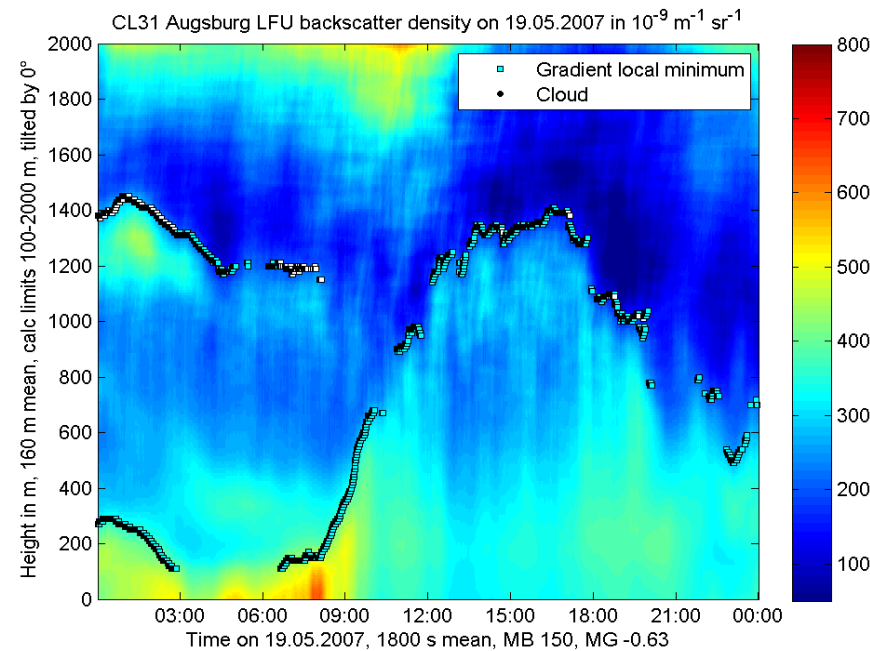
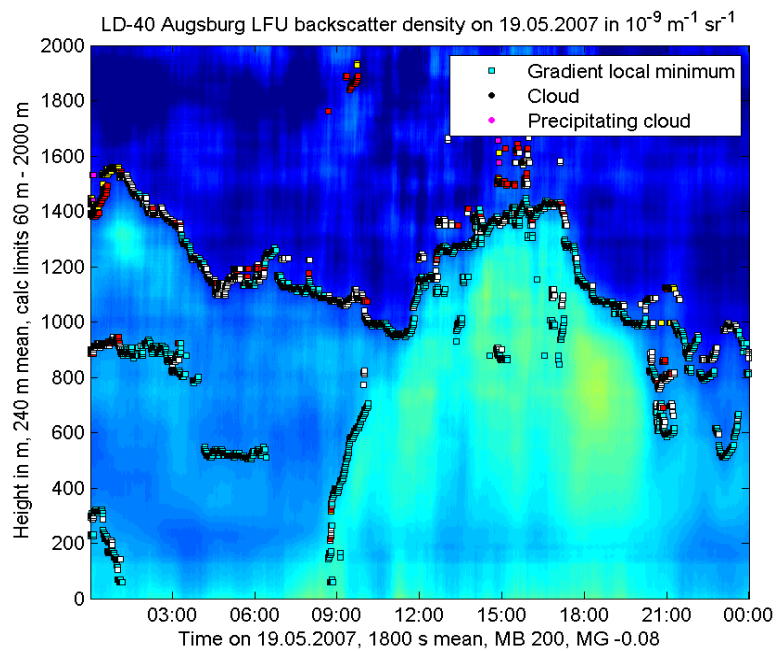
wave length: 905 nm

height resolution: 5 m

max. range: 7500 m



19 May 2007: ceilometer LD40 and CL31

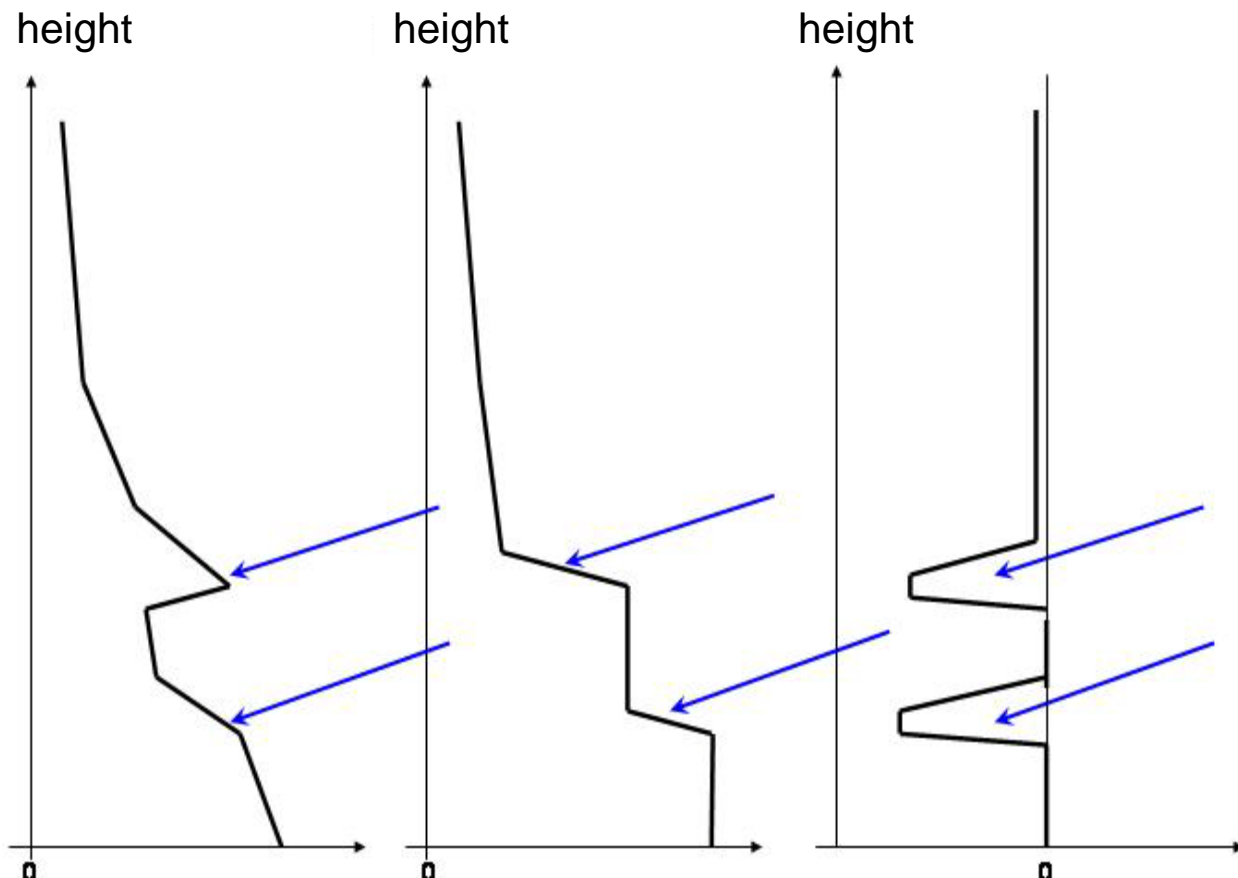


Comparison SODAR and Ceilometer

comparison of
algorithms

left: SODAR

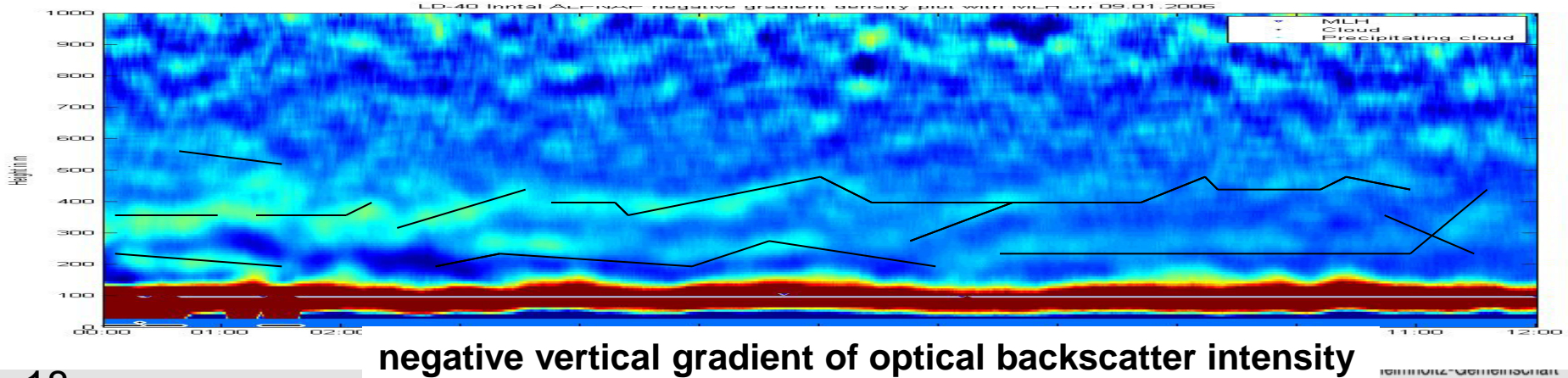
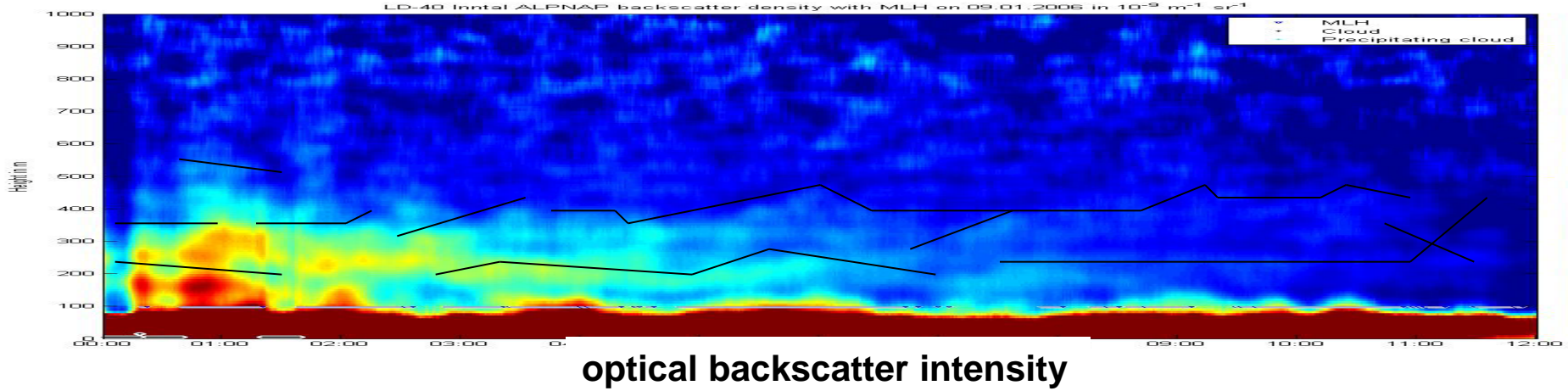
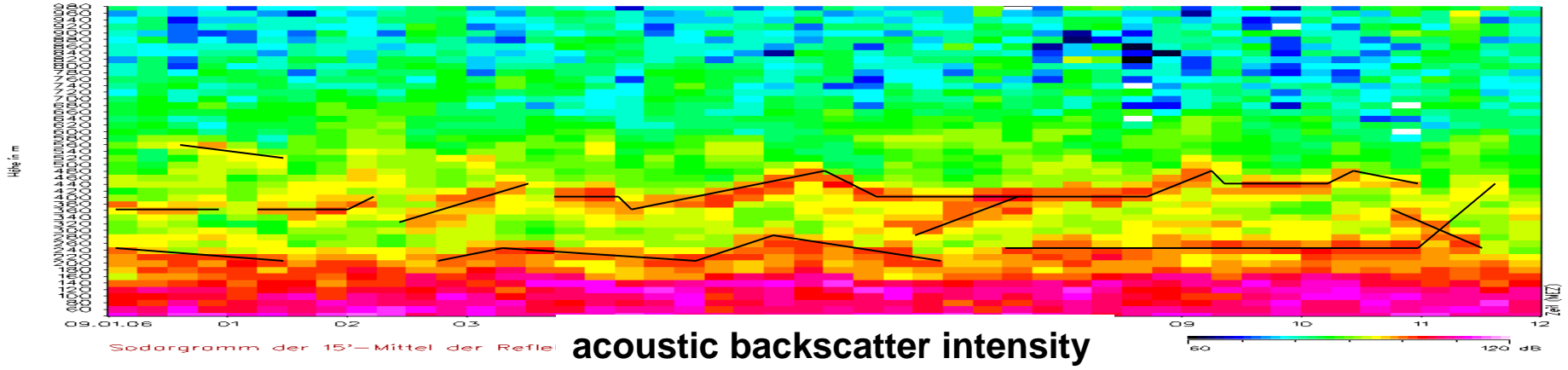
middle and right:
ceilometer



acoustic backscatter
intensity

optical backscatter
intensity

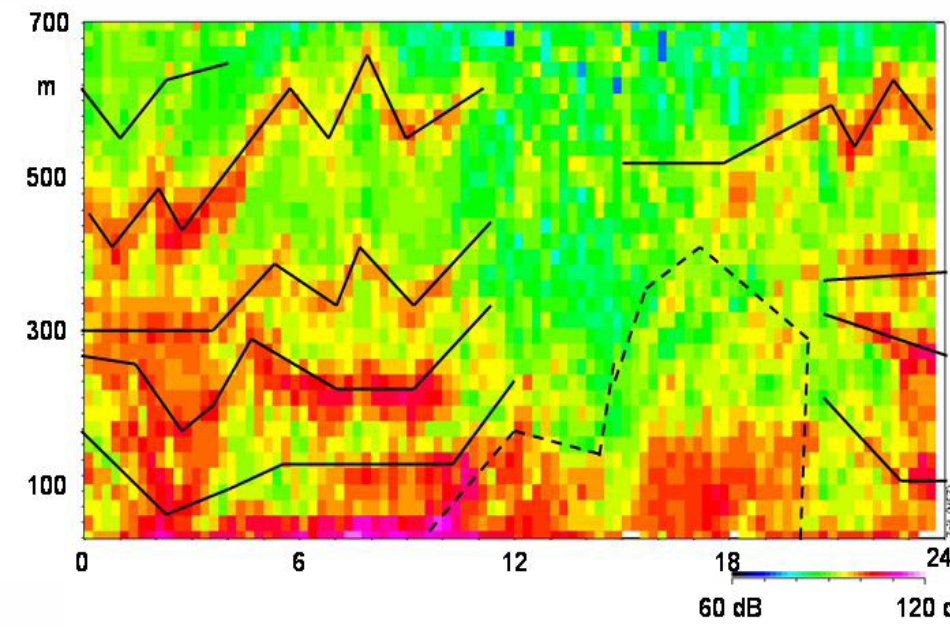
vertical gradient of
optical backscatter
intensity



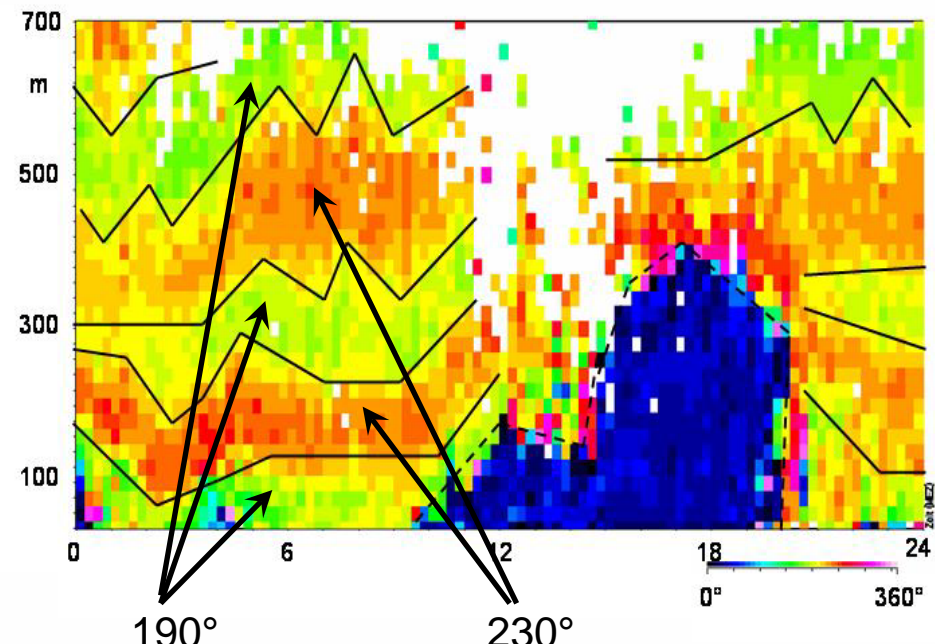
Application examples for SODAR and Ceilometer

SODAR measurements in a wintry Alpine valley

29 January 2006

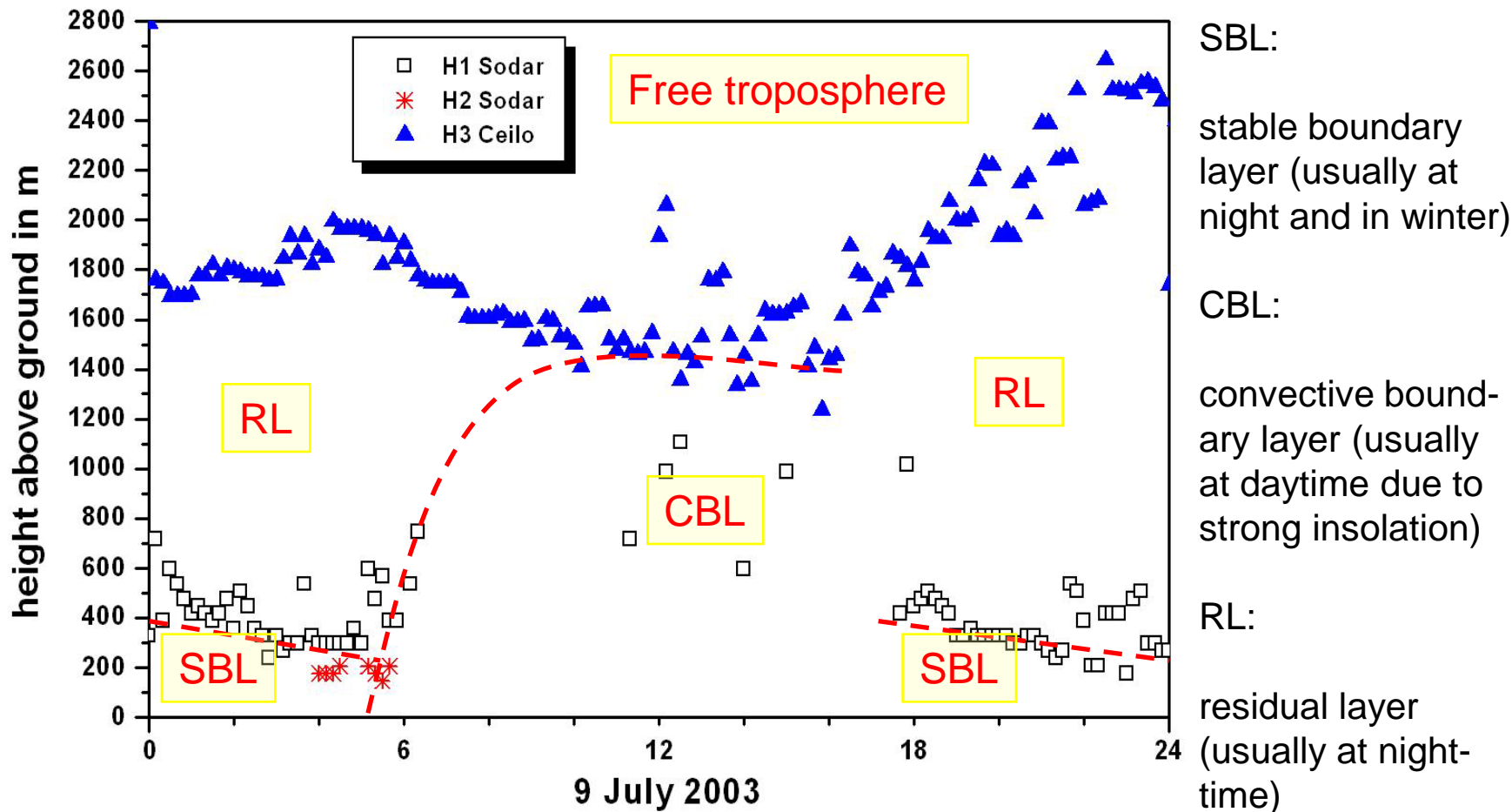


backscatter intensity

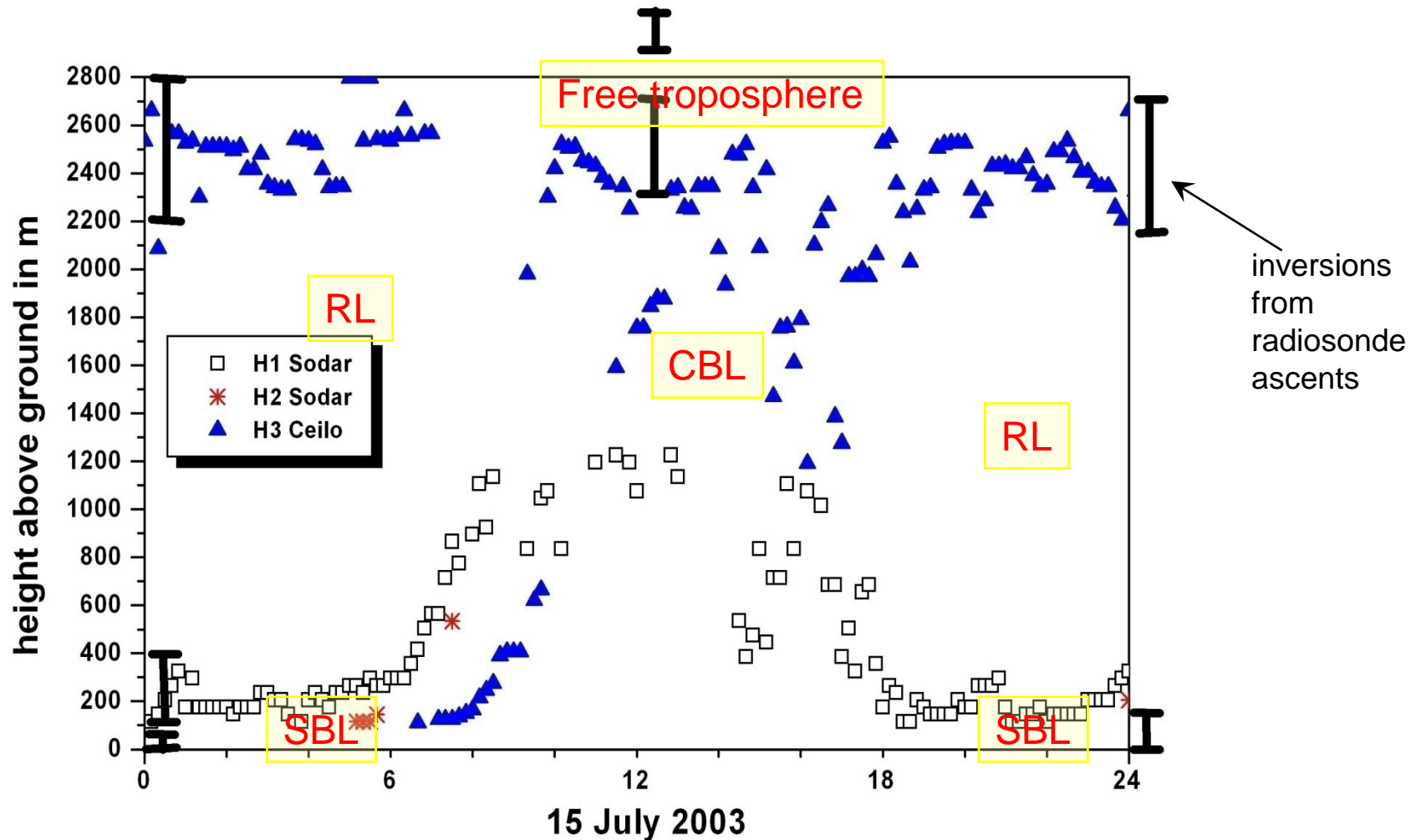


wind direction

Diurnal variation of mixing-layer height from SODAR and Ceilometer data (Budapest)

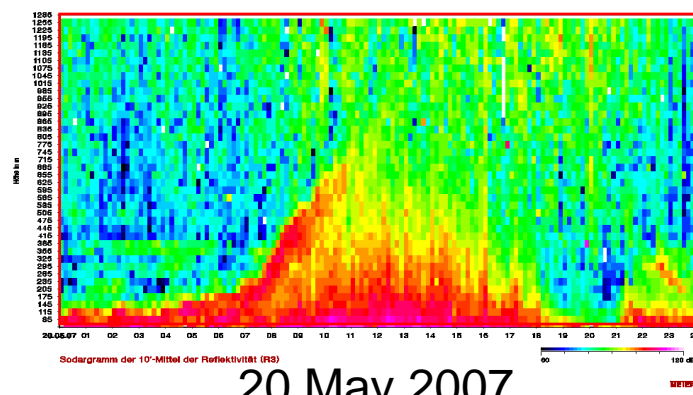
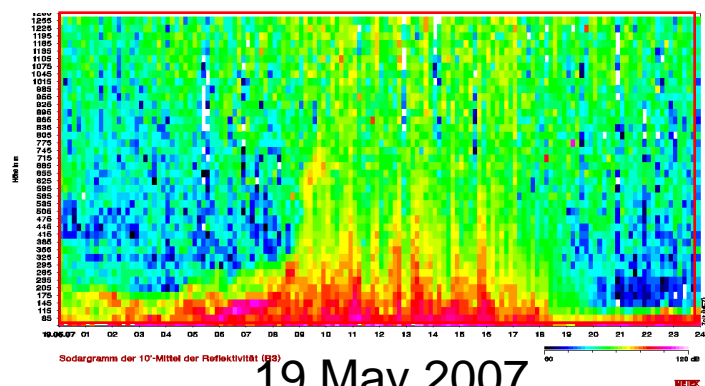
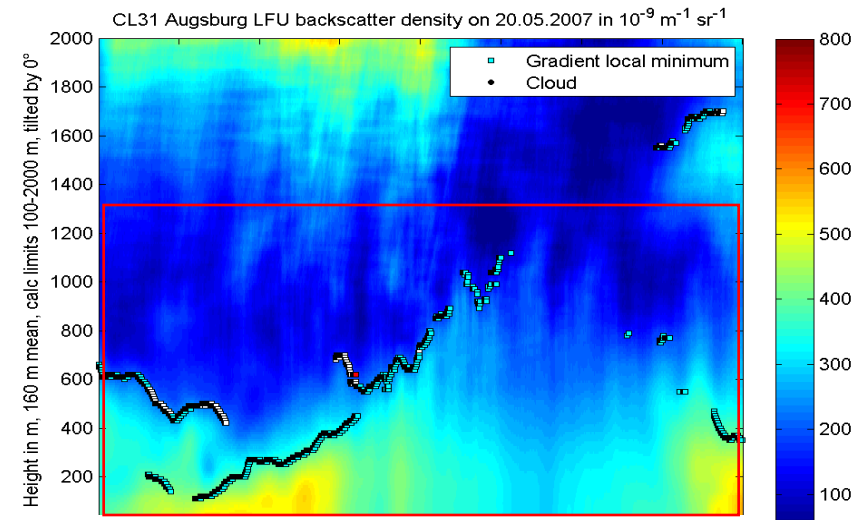
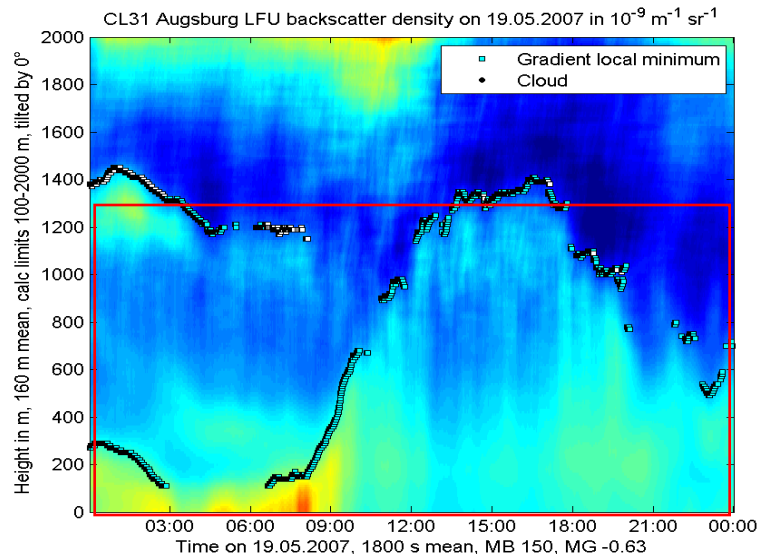


Simultaneous operation SODAR-Ceilometer: examples for summer days

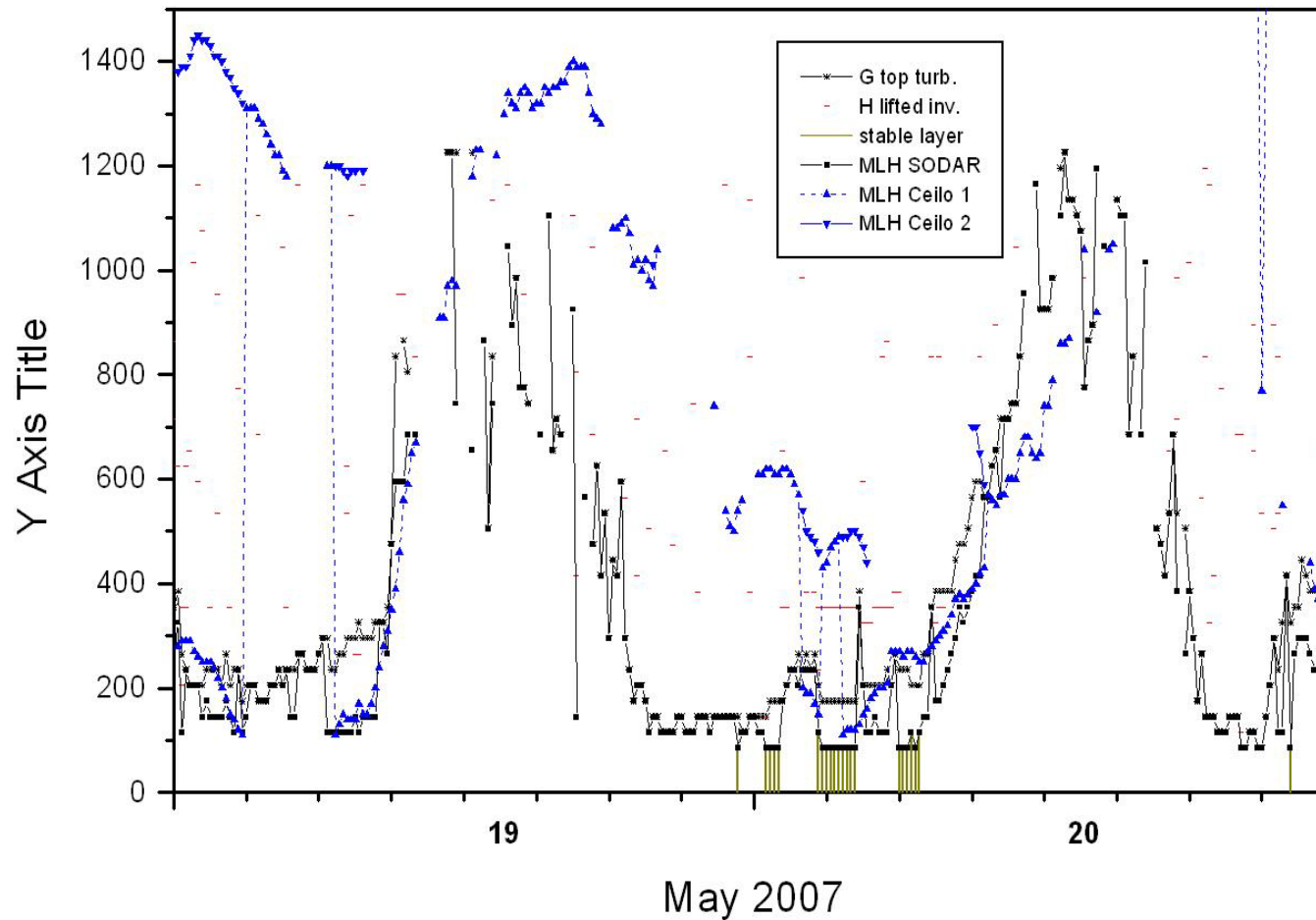


Emeis, S., K. Schäfer, 2006: Remote sensing methods to investigate boundary-layer structures relevant to air pollution in cities.
 Bound.-Lay Meteorol., 121, 377-385,

comparison of optical (top) and acoustic (below) backscatter intensity



comparison of MLH from Sodar and CL31 data



RASS

principles of operation

examples

RASS (radio-acoustic remote sensing)

measures vertical temperature profiles

Bragg-RASS: windprofiler plus acoustic component

Doppler-RASS: SODAR plus electro-magnetic component

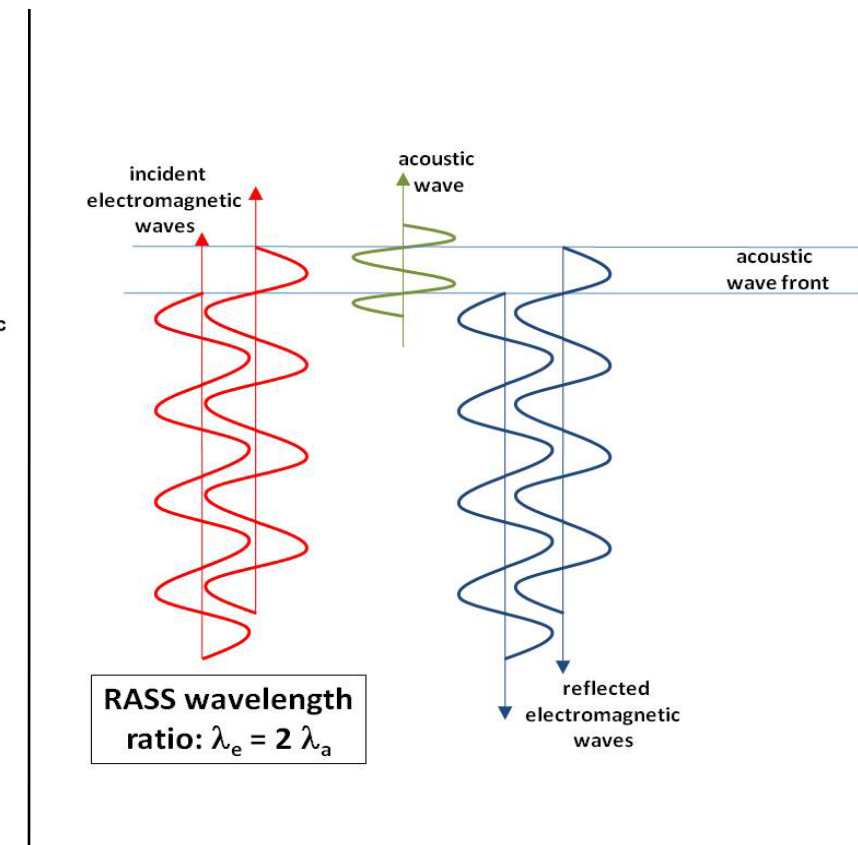
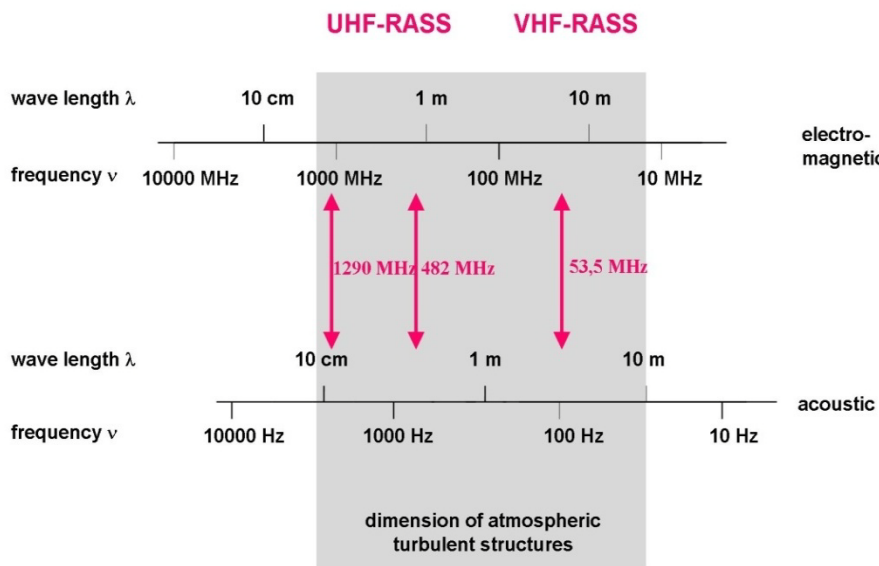
UHF RASS (boundary layer)

VHF RASS (troposphere)

RASS: frequencies

Bragg condition:
acoustic wavelength = $\frac{1}{2}$ electro-magnetic wavelength

electro-magnetic - acoustic frequency pairs for RASS devices





SODAR-RASS (Doppler-RASS)

(METEK)

acoustic frequ.: 1500 – 2200 Hz

radio frequ.: 474 MHz

resolution: 20 m

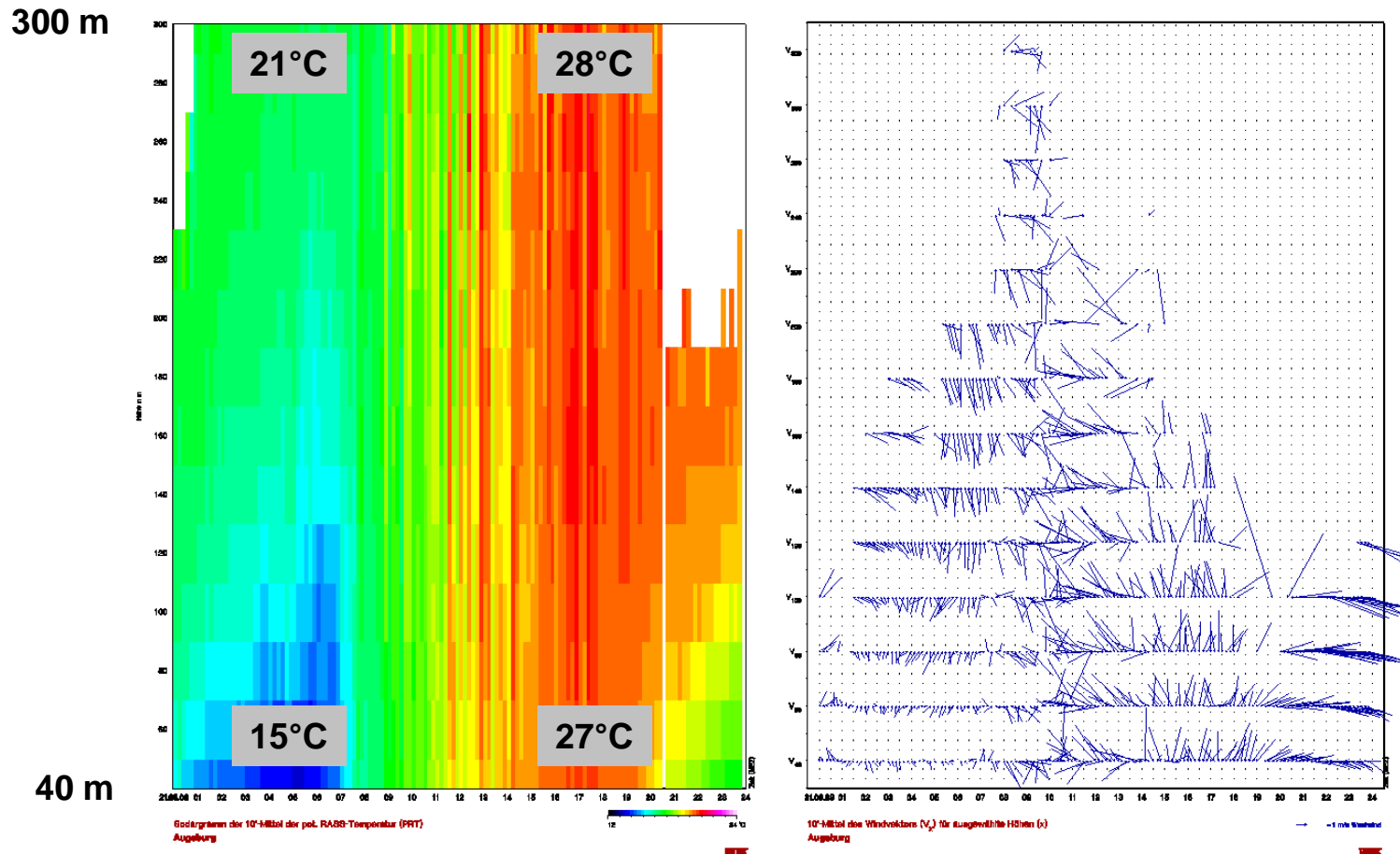
lowest

range gate: ca. 40 m

vertical range: 540 m

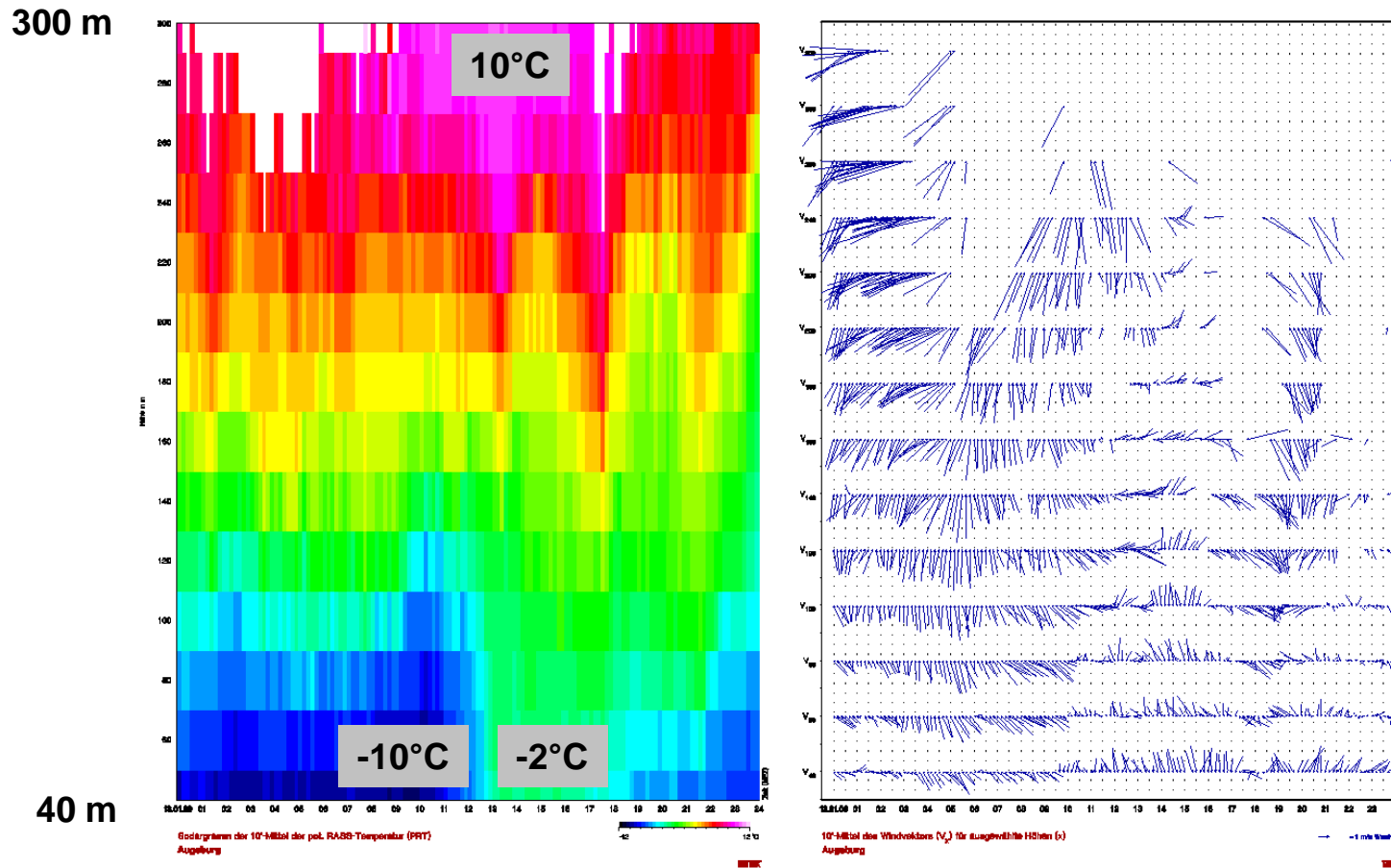
temperature profile and dynamics

example RASS data: summer day
potential temperature (left), horizontal wind (right)



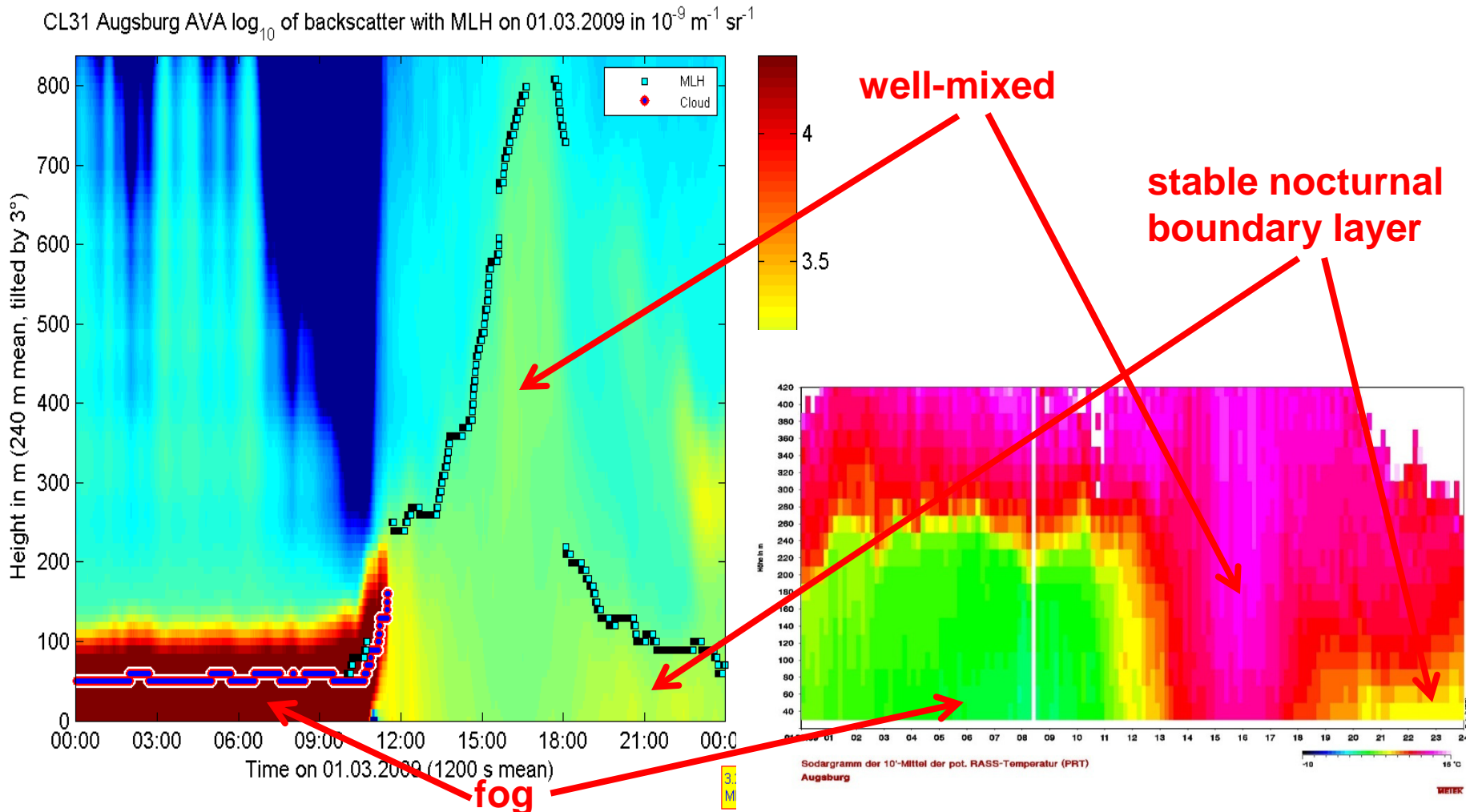
temperature profile and dynamics

example RASS data: winter day
potential temperature (left), horizontal wind (right)



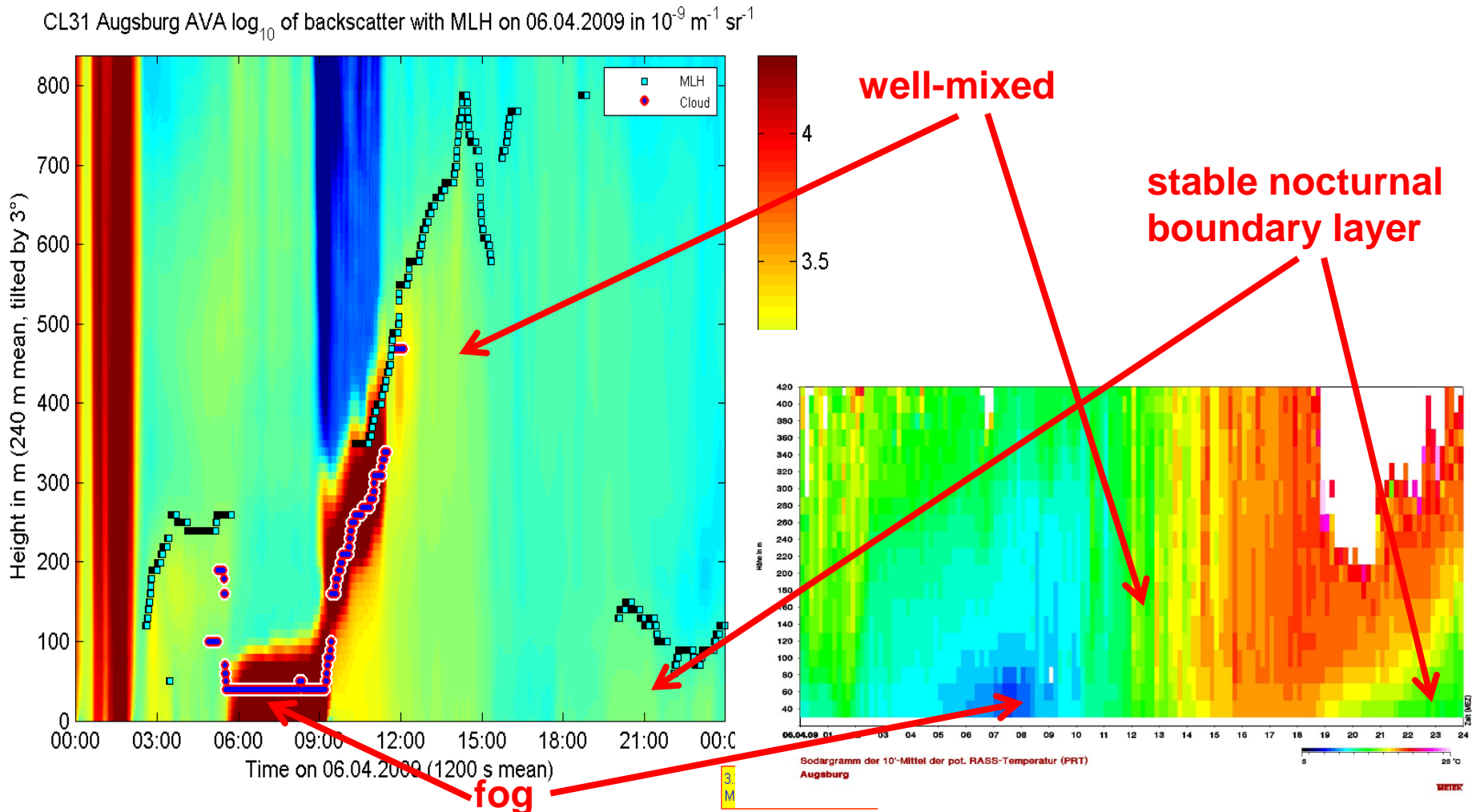
temperature profile and pollution

comparison of RASS data (potential temperature, right)
with aerosol backscatter from a ceilometer (left)



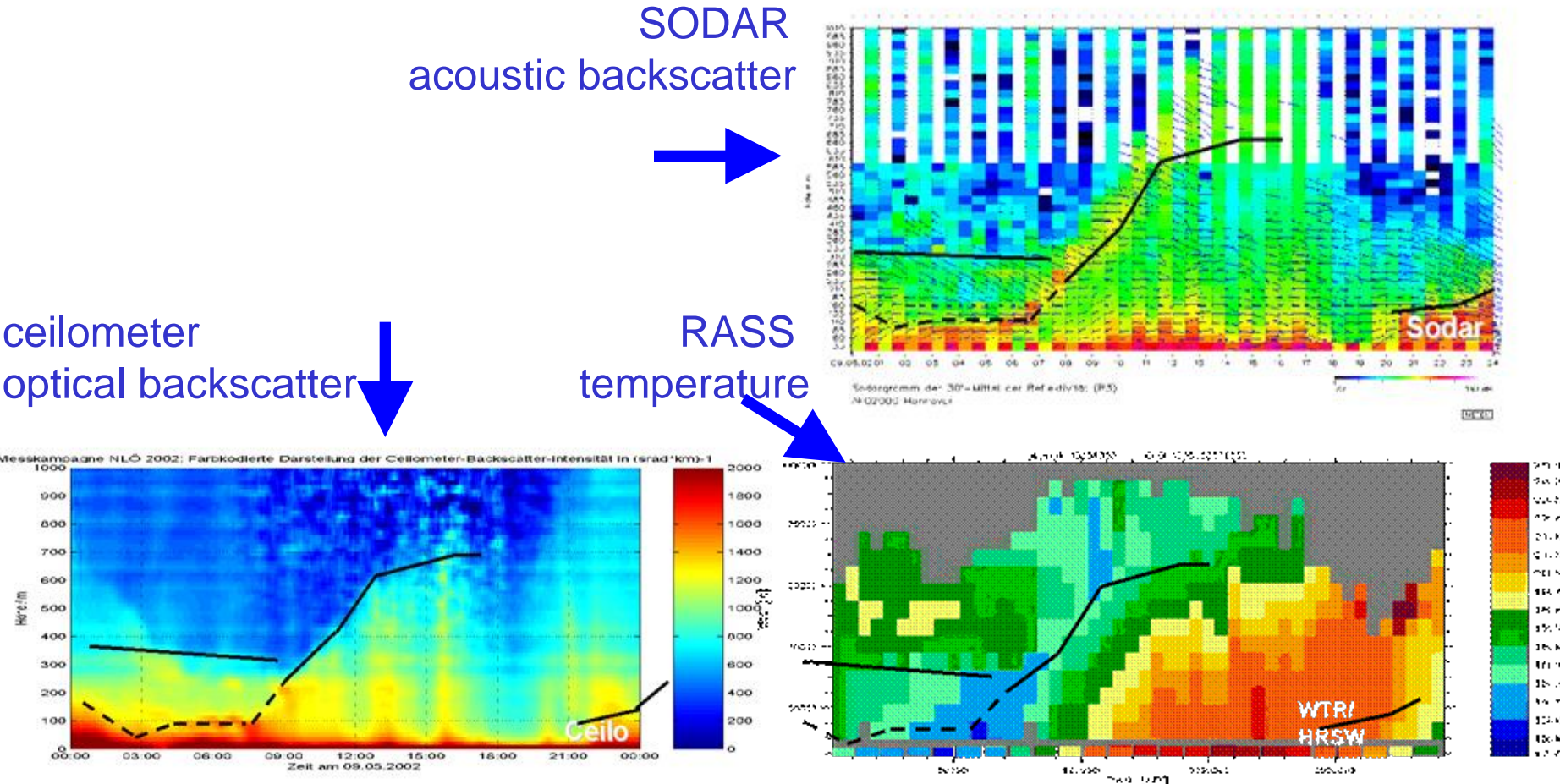
temperature profile and pollution

comparison of RASS data (potential temperature, right)
with aerosol backscatter from a ceilometer (left)



Summary

Comparison of MLH retrievals with three different remote sensing techniques



Emeis, S., Chr. Münkel, S. Vogt, W.J. Müller, K. Schäfer, 2004: Atmospheric boundary-layer structure from simultaneous SODAR, RASS, and ceilometer measurements. *Atmos. Environ.*, 38, 273-286.

Overview on methods using ground-based remote sensing for the derivation of the mixing-layer height

method	short description
acoustic ARE method	analysis of acoustic received echo intensity profiles
“ HWS method	analysis of horizontal wind speed profiles
“ VWV method	analysis of vertical wind variance profiles
“ EARE method	analysis of acoustic backscatter intensity and vertical wind variance profiles (enhanced acoustic received echo method)
optical threshold method	detection of a given backscatter intensity threshold
“ gradient method	analysis of optical backscatter intensity profiles
“ idealised backscatter method	analysis of optical backscatter intensity profiles
“ wavelet method	analysis of optical backscatter intensity profiles
“ variance method	analysis of optical backscatter intensity profiles
acoustic / electro-magnetic	ARE method applied to sodar and wind profiler data
acoustic / optical	EARE method plus gradient method
electro-magnetic / electro-magnetic	combination of a sodar-RASS and a wind profiler RASS: analysis of the vertical temperature profile plus analysis of the electro-magnetic backscatter intensity profile
acoustic / in situ	ARE method plus in-situ surface flux measurement
RASS	analysis of the temperature profile from the measured speed of sound

Conclusions:

RASS directly delivers temperature profiles,
MLH, inversions, and stable layers can easily be detected,
wind profiles are additionally available.
Does not work properly with high wind speeds.

SODAR detects temperature fluctuations and gradients,
but no absolute temperature. Inversions and stable layers can
indirectly be inferred with a MLH algorithm.
Does not work properly with perfectly neutral stratification, with
very high wind speeds, and during stronger precipitation events.

Ceilometer detects aerosol distribution and water droplets. It has
to be assumed that the aerosol follows the thermal structure of
the atmosphere. Inversions and MLH can indirectly be inferred
with a MLH algorithm.
Does not work properly in extreme clear (aerosol-free) air and
during precipitation events and fog.

Literature

SODAR:

Asimakopoulos, D.N., C.G. Helmis, J. Michopoulos, 2004: Evaluation of SODAR methods for the determination of the atmospheric boundary layer mixing height. - *Meteor. Atmos. Phys.* 85, 85–92.

Beyrich, F., 1997: Mixing height estimation from sodar data – a critical discussion. - *Atmos. Environ.* 31, 3941–3953.

Ceilometer:

Schäfer, K., S.M. Emeis, A. Rauch, C. Münkel, S. Vogt, 2004: Determination of mixing-layer heights from ceilometer data. In: *Remote Sensing of Clouds and the Atmosphere IX*. Schäfer, K., A. Comerón, M. Carleer, R.H. Picard, N. Sifakis (Eds.), Proc. SPIE, Bellingham, WA, USA, Vol. 5571, 248–259.

Sicard, M., C. Pérez, F. Rocadenbosch, J.M. Baldasano, D. García-Vizcaino, 2006: Mixed-Layer Depth Determination in the Barcelona Coastal Area From Regular Lidar Measurements: Methods, Results and Limitations. - *Bound.-Lay. Meteor.* 119, 135–157.

RASS:

Engelbart, D.A.M., J. Bange, 2002: Determination of boundary-layer parameters using wind profiler/RASS and sodar/RASS in the frame of the LITFASS project. *Theor. Appl. Climatol.* 73, 53–65.

Emeis, S., K. Schäfer, C. Münkel, 2009: Observation of the structure of the urban boundary layer with different ceilometers and validation by RASS data. *Meteorol. Z.*, 18, 149-154. ([Open access, freely available from http://dx.doi.org/10.1127/0941-2948/2009/0365](#))

Reviews:

Emeis, S., K. Schäfer, C. Münkel, 2008: Surface-based remote sensing of the mixing-layer height – a review. - *Meteorol. Z.*, 17, 621-630. ([Open access, freely available from http://dx.doi.org/10.1127/0941-2948/2008/0312](#))

Emeis, S., M. Harris, R.M. Banta, 2007: Boundary-layer anemometry by optical remote sensing for wind energy applications. - *Meteorol. Z.*, 16, 337-347.